Putting Water on a Lattice: The Importance of Long Wavelength Density Fluctuations in Theories of Hydrophobic and Interfacial Phenomena

Suriyanarayanan Vaikuntanathan[1] and Phillip L. Geissler[1,2]
[1]Material Sciences Division, Lawrence Berkeley National Laboratory, Berkeley, California 94720, USA
[2]Department of Chemistry, University of California, Berkeley, California 94720, USA
(Received 29 July 2013; published 15 January 2014)

The physics of air-water interfaces plays a central role in modern theories of the hydrophobic effect. Implementing these theories, however, has been hampered by the difficulty of addressing fluctuations in the shape of such soft interfaces. We show that this challenge is a fundamental consequence of mapping long wavelength density variations onto discrete degrees of freedom. Drawing from studies of surface roughness in lattice models, we account for the resulting nonlinearities simply but accurately. Simulations show that this approach captures complex solvation behaviors quantitatively.

DOI: 10.1103/PhysRevLett.112.020603 PACS numbers: 05.20.Jj, 61.20.Ja, 64.60.De, 68.03.Kn

The fluctuating roughness of liquid-vapor interfaces spans a wide range of length scales [1]: from the mesoscopic, where the coarse view of capillary wave theory is appropriate [2], to the microscopic [3,4], where molecular considerations are essential. These topographical fluctuations can impact an equally broad spectrum of physical responses, with important implications for behaviors of modern interest in biophysics, chemical physics, and materials science including the binding of ligands to hydrophobic protein cavities [5], self-assembly of nanoparticles at interfaces [6], and the affinity of diverse solutes for the liquid's boundary [7–9]. Lum, Chandler, and Weeks (LCW) developed a comprehensive conceptual framework for linking such phenomena to fluctuations in the liquid's microscopic density field [10], to which surface roughness clearly contributes. Computer simulations of LCW-inspired models, which simultaneously address fluctuations at fine and coarse scales, have been used to understand many basic aspects of hydrophobic solvation and self-assembly [11–15]. The treatment of long wavelength ($\gtrsim$1 nm) density fluctuations in many of these approaches, however, has fallen short of quantitative accuracy due to the difficulties associated with representing smoothly varying fields in a model amenable to simulation [12]. As a result, they have not been free of potentially significant lattice artifacts or else the need to introduce parameters that are poorly constrained by available data [12,16].

In this Letter, we show that previous difficulties in modeling coarse variations in liquid density reflect the rich statistical physics of discretely fluctuating surfaces, whose relevance in this context has not been elaborated. In particular, the component of the density field that varies slowly in space is naturally described in numerical approaches by a lattice model. This choice of a discrete representation introduces profound nonlinearities, which can cause decoupling of notionally equivalent measures of surface tension. In extreme cases, these nonlinearities can even drive a phase transition from a rough to a quiescent state [18], which lacks the long wavelength fluctuations altogether.

The basic physics emerging from these nonlinearities has been plumbed in other contexts [18–20]. Here, we exploit and extend the resulting understanding and its connection with the molecular physics of microscopic density fluctuations. Specifically, through an analysis of the lattice gas model [Eq. (1)] and related approximations [Eq. (3)], we identify a narrow parameter regime in which the lattice gas model can optimally be used to describe long wavelength liquid density fluctuations such as the capillary modes [2,16] at a liquid-vapor interface. Coupling fluctuations in the lattice model to fluctuations on finer molecular scales through the least complicated realization of the LCW perspective, we then obtain an effective Hamiltonian [Eq. (6)] for lattice occupation variables in the presence of a hydrophobic solute. We show that this Hamiltonian—with no unknown parameters—in fact suffices to describe quantitatively the solvation of hydrophobic objects with various shapes and sizes. This success establishes a minimally complicated model for the hydrophobic effect that is faithful to the intrinsic softness of the air-water interface. It further allows us to parse contributions from various length scales to material properties of the liquid-vapor interface, such as the Tolman length, bending rigidity, and spontaneous curvature. This model is uniquely well suited for exploring hydrophobic and interfacial phenomena that involve disparate length scales, e.g., association of hydrophobic solutes with interfaces [5,21], solvation of large hydrophobic objects with microscopic features, and the growth of hydrophobic assemblies beyond the nanometer scale.

Lattice gas analysis.—The stability of a macroscopic liquid-vapor interface originates in the statistical mechanics of phase transitions. Classic descriptions of long wavelength variations in that context include phenomenological theories for smooth fields [23] and schematic lattice models that implicitly perform coarse graining over scales smaller

than a lattice spacing l [2,11]. The latter involve a minimum of parameters (as few as l and an energy scale ϵ of microscopic cohesion) and are particularly convenient for numerical simulation. We, like others [2,11], therefore focus on such a discrete representation, where n_i indicates the molecular density within lattice cell i in a binary way: $n_i = 1$ and $n_i = 0$ denote locally liquidlike and vaporlike density, respectively. Fluctuations of these occupation variables are governed by a lattice gas Hamiltonian,

$$H = -\epsilon \sum_{\langle i,j \rangle} n_i n_j - \mu \sum_i n_i, \tag{1}$$

where $\sum_{\langle i,j \rangle}$ denotes a sum over nearest neighbor cells and μ is the chemical potential. We have in mind systems such as ambient water that are close to coexistence, $\mu \approx -3\epsilon + \Delta P l^3$, where $\Delta P \gtrsim T/l^3$ is the difference between ambient pressure and the liquid's vapor pressure, and T is given in units of k_B.

How the parameters l and ϵ should be assigned for a particular material is a surprisingly subtle and pivotal issue. Previous work has argued that l should correspond to the correlation length of density fluctuations in the liquid phase [11]. We are concerned with fluids far below their critical points, setting this length scale slightly in excess of a molecular diameter ($l \approx 4$ Å in liquid water). The energy scale ϵ was inferred from the cost of creating an interface at zero temperature. Equating this cost with the free energy per unit area Γ of a real liquid interface at finite temperature yields [11]

$$\Gamma = \frac{\epsilon}{2l^2}. \tag{2}$$

According to these arguments, $\epsilon \approx 6.0T$, in the case of water at ambient conditions. We will show that such a high value is problematic.

While this reasoning is sensible, it entirely neglects the influence of interfacial fluctuations. To account for these shape variations, we consider a macroscopically planar, fluctuating interface between liquid and vapor phases, within the so-called solid-on-solid (SOS) limit [2,24–27]. In this approximation the two phases are each assumed to be internally homogeneous: $n_i = 1$ everywhere in the liquid phase and $n_i = 0$ everywhere in the vapor, as roughly expected far from criticality. Any configuration of this sort can be specified by the height h_i of the liquid phase in each column i of the lattice (taking the interface to be horizontal, with liquid below). At coexistence and within the SOS approximation, the Hamiltonian Eq. (1) can thus be rewritten as [25]

$$H_0 = \frac{\epsilon}{4l} \sum_{\langle i,j \rangle} |h_i - h_j|. \tag{3}$$

The SOS limit of Eq. (1), Eq. (3), has often been used to investigate the interfacial properties of the lattice gas [2,25].

Our strategy is to estimate the spectrum of capillary waves for the SOS limit of the lattice gas (at finite temperature) and enforce agreement with that of water. According to capillary wave theory, the Fourier modes $\hat{h}(\mathbf{q})$ of a continuous interface fluctuate with squared amplitude $\langle |\hat{h}(\mathbf{q})|^2 \rangle \propto 1/\gamma_{\rm cap} q^2$, where $\gamma_{\rm cap}$ denotes the surface tension governing capillary fluctuations. Molecular simulations [12] and experiments [28] indicate that modes of the air-water interface with wavelength $2\pi/q \gtrsim 1$ nm indeed follow this scaling and that $\gamma_{\rm cap}$ corresponds closely with the thermodynamic surface tension Γ [12,29]. Capillary wave scaling does not necessarily hold for the lattice gas model, whose interfacial roughness depends on temperature in subtle ways [18,30].

In order to relate $\gamma_{\rm cap}$ and ϵ for the lattice gas in the SOS limit, we ignore for the moment the discrete nature of fluctuations and variationally seek the most representative Gaussian model $H_{\rm cap} = \gamma_{\rm cap}/(4l^2) \sum_{\langle i,j \rangle} (h_i - h_j)^2$. According to the Gibbs's variational principle,

$$F_0 \leq F_{\rm cap} + \langle H_0 - H_{\rm cap} \rangle_{\rm cap}, \tag{4}$$

where $\langle \ldots \rangle_{\rm cap}$ denotes an average taken with respect to the Hamiltonian $H_{\rm cap}$, $F_{\rm cap}$ denotes the free energy corresponding to $H_{\rm cap}$, and F_0 denotes the free energy corresponding to the SOS limit of the lattice gas, H_0. This bound yields an optimal parametrization (see the Supplemental Material [17] for derivation)

$$\beta \gamma_{\rm cap} = \frac{(\beta\epsilon)^2}{\pi l^2}, \tag{5}$$

where $\beta = 1/T$. This result, scaling quadratically with ϵ, is clearly distinct from the low-temperature relationship in Eq. (2). We performed numerical simulations of the SOS model with values of ϵ/T in the range $0.4 \leq \epsilon/T \leq 1.6$ and found the variational estimate to be very accurate for $\epsilon/T \lesssim 1.4$ (see Fig. 1 and the Supplemental Material [17]). Comparison with the lattice gas is favorable over a more limited range, since the SOS approximation breaks down at low values of ϵ as the critical point $\epsilon_c/T \approx 0.89$ is approached. Specifically, the range over which the capillary surface tension predicted by Eq. (5) mirrors that of the lattice gas is roughly bounded on the lower end by $\epsilon \gtrsim 1.25T$. We obtain this lower bound by computing $\gamma_{\rm cap}$ for the lattice gas model at coexistence [31] and comparing these estimates to those predicted by Eq. (5) (see Supplemental Material [17]). We will argue that the range $1.25 \lesssim \epsilon/T \lesssim 1.40$ is ideal for representing liquid-vapor interfaces.

The breakdown of our variational estimate at high values of ϵ/T reflects a well-known singularity in the statistical physics of discretely fluctuating surfaces [18,19]. Above a critical value $\epsilon_R/T \approx 1.63$, roughness of the SOS surface is markedly suppressed [18]. This transition to a quiescent interface, which lacks capillary wave scaling, is generic to

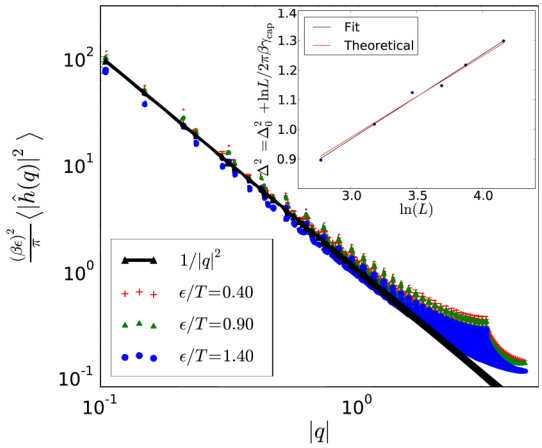

FIG. 1 (color online). (Log-log) plots of $(\beta\epsilon)^2\langle|\hat{h}(q)|^2\rangle/\pi$, where $\hat{h}(q)$ denotes the Fourier modes of interfacial fluctuations in a solid-on-solid model. Over a fairly large range of the lattice coupling strength ϵ/T, this plot demonstrates that $(\beta\epsilon)^2\langle|\hat{h}(q)|^2\rangle/\pi \approx 1/|q|^2$ for small values of $|q|$, thus verifying the scaling predicted in Eq. (5). Inset: capillary fluctuations of the lattice gas, at $\epsilon/T = 1.35$. The squared interfacial thickness Δ^2 determined from simulations depends logarithmically on the lateral dimension L, as predicted by capillary wave theory. The proportionality coefficient for this dependence indicates the surface tension γ_{cap}. The value extracted by fitting simulation results (Supplemental Material [17]) agrees well with predictions of Eq. (5). The height h_i, the interfacial width Δ, and L are given in lattice units here.

models that feature a minimum energetic penalty for local deviations from flatness [18,19]. Our variational estimate breaks down for values of ϵ/T noticeably below the roughening value. For values of ϵ/T below but close to the roughening transition, the discrete constraints on lattice fluctuations, which we have ignored while deriving Eq. (5), become relevant and $\beta\gamma_{\mathrm{cap}} \neq (\beta\epsilon)^2/(\pi l^2)$. Their effects can approximately be assessed by following Ref. [19] and adding a potential $V_0 \equiv -2y_0\epsilon\sum_i \cos(2\pi h_i)$ to the optimal Gaussian variation Hamiltonian with Eq. (5). This potential penalizes configurations in which height fluctuations deviate from discrete values [19] with the constant y_0 determining the strength of this penalty. Standard methods [19,20] can be used to calculate the corresponding renormalized surface tension γ_{cap}. We choose y_0 so that the value of ϵ/T at which this modified system undergoes a roughening transition is close to that of the SOS lattice. We then find that for $\epsilon/T \lesssim 1.4$ there is no significant renormalization due to the discrete constraints (see Supplemental Material [17]).

On the basis of this analysis, we argue that the range of lattice gas parameters consistent with the physics of hydrophobic solvation is quite narrow. Large hydrophobic objects induce local drying, generating microscopic analogs of a macroscopic interface between liquid and vapor. Faithfully capturing fluctuations of such microscopic interfaces requires that ϵ be smaller than the critical value for roughening of the lattice gas interface $\epsilon < \epsilon_R$ [18]. For values of ϵ slightly below ϵ_R, the discrete nature of the lattice does not entirely suppress long wavelength capillary modes, but it nonetheless significantly influences the statistics of surface fluctuations. For example, the surface tension of the lattice gas is anisotropic in this regime [30], depending on the orientation of the interface with respect to the axes of the cubic lattice. The implications of this and related lattice artifacts for solvation behaviors of convex objects on cubic lattices have been discussed previously [12,32]. They encourage using lattice coupling energies that are weaker still, $\epsilon/T \lesssim 1.4$, for which discreteness is an unimportant feature.

The SOS approximation, which relies upon spatial uniformity within each phase, is well motivated for liquid water at ambient conditions. Here, and in most liquids near their triple points, spontaneous density fluctuations away from the average bulk value ρ_l are typically small even on molecular length scales. The range of cohesive energies $1.25T \lesssim \epsilon \lesssim 1.4T$ for which the variational estimate in Eq. (5) is faithful is hence also optimal to represent fluctuations in real, far-from-critical liquids. Through Eq. (5), this range of cohesive energies implies a correspondingly narrow range of appropriate lattice spacing l. In the case of water, using the experimental value of surface tension [12] $\gamma_{\mathrm{cap}} \approx 17.4T/\mathrm{nm}^2 = \epsilon^2/(\pi l^2)$, this coarse graining length should, according to our arguments, lie between 1.7 and 1.9 Å. Some previous work has adopted values of l close to this range [15] but in each case has assigned an energy scale through the low-temperature relationship Eq. (2).

Incorporating fine scale fluctuations through the LCW perspective.—Having tightly constrained the possible choices of ϵ and l, we focus on implications for the theory and modeling of aqueous solutions: Can a suitably parametrized lattice model for long wavelength variations in density, together with a simple theory for molecular scale fluctuations, accurately predict nontrivial solvation behavior? To do so, we employ the LCW perspective in its simplest incarnation, put forth in Ref. [10]. Locally liquidlike regions ($n_i = 1$) additionally support short wavelength density fluctuations that are assumed to obey Gaussian statistics [3], as characterized by the two-point correlation function $\chi(\mathbf{r}-\mathbf{r}') = \rho_l\delta(\mathbf{r}-\mathbf{r}') + \rho_l^2(g(\mathbf{r}-\mathbf{r}')-1)$, where $g(r)$ denotes the radial distribution function [23].

We consider solutes that are ideally hydrophobic, whose sole influence is to exclude solvent from a volume v. The constraint of solvent evacuation within a lattice cell i can be accommodated either through variation in the slowly varying density field ($n_i = 0$) or through a variation in the above mentioned short wavelength Gaussian density field in a locally liquidlike region. Integrating out short wavelength fluctuations yields an effective Hamiltonian for lattice occupation variables in the presence of a solute [11,12]

$$H_v[n_i] = -\epsilon \sum_{\langle i,j \rangle} n_i n_j - \mu \sum n_i + T\left[\frac{\langle N_v \rangle^2}{2\sigma_v}\right] + \frac{TC}{2}, \quad (6)$$

$$\langle N_v \rangle = \Sigma_i \rho_l n_i v_i, \quad \sigma_v = \int_{\mathbf{r}\in v}\int_{\mathbf{r}'\in v} \Theta(\mathbf{r})\chi(\mathbf{r},\mathbf{r}')\Theta(\mathbf{r}'), \quad (7)$$

where

$$C = \begin{cases} \ln\,(2\pi\sigma_v) & \text{if} \langle N \rangle_v > 1\,, \\ \max\,[\ln\,(2\pi\sigma_v), \langle N \rangle_v] & \text{otherwise}, \end{cases} \quad (8)$$

and $\Theta(\mathbf{r}) = 1$ if the lattice cell containing $\mathbf{r}$ is occupied and vanishes otherwise, and v_i is the volume of overlap between v and lattice cell i. The coarse-grained model defined by Eq. (6) includes as free parameters only the energy and length scales of the underlying lattice gas, which we set as $\epsilon = 1.35T$, and consistent with the statistical mechanics of rough interfaces [Eq. (5)], $l = 1.84$ Å (see inset, Fig. 1). We used $\mu = -3\epsilon + 1.51 \times 10^{-4}T$ [15] for these simulations. Note that the only inputs to this theory are the surface tension of water and its pair correlation $g(r)$ [23].

Simulations.—Using Monte Carlo simulations of this coarse-grained description, we computed the reversible work F required to transfer volume-excluding solutes from vapor into the bulk liquid phase (see the Supplemental Material [17]). We focus first on spherical hydrophobes, for which solubility has been previously determined as a function of radius R from detailed molecular simulations [33]. The free energy per unit solute surface area $A = 4\pi R^2$ is plotted in Fig. 2(a)(1). Results for the lattice model agree very well with simulation data. As a more stringent test, we computed solvation free energies for hydrophobic objects that vary not only in scale but also in shape. It is not obvious whether a microscopic sphere with given surface area should differ substantially in solubility from, e.g., a cube with the same area. As shown in Fig. 2(a), solvation properties can in fact be very sensitive to such geometric details. For all of the shapes we considered (spheres, cubes, and cuboids), F/A grows rapidly as radius R (or edge length L for the cubes and cuboids considered here) grows to ~1 nm, then increases much more gradually at larger R (or L) value. The details of this dependence, however, differ significantly. A naive extrapolation could even suggest that F/A approaches different limiting values at large R for different shapes. These behaviors are observed in molecular simulations [using the SPC/E model of water (see the Supplemental Material [17])] and for the coarse-grained theory of Eq. (6), with remarkably close correspondence between the two approaches. From the solubility of cubic volumes, we extract the thermodynamic surface tension $\Gamma = 14.92T/\text{nm}^2$ of our lattice model by extrapolating to $L^{-1} \to 0$ [see Fig. 2(b)].

The sensitivity of a hydrophobe's solubility to its shape reflects properties of liquid-vapor interfaces that are more subtle than macroscopic surface tension (i.e., Γ or γ_{cap}). Corresponding material parameters are conventionally defined in terms of an expansion in powers of curvature $1/R$. The Tolman length δ, for example, is defined according to $F_{\text{sph}}/A = \Gamma(1 - 2\delta/R + \cdots)$. A more directly mechanical view is provided by mapping this curvature-dependent response onto that of an elastic sheet. According to Helfrich's phenomenological theory, the elastic free energy of a thin shell with bending rigidity κ and spontaneous curvature c_0 is given by [34]

$$\frac{F_{\text{sph}}}{A} = \Gamma - \frac{4\kappa c_0}{R} + C_1\frac{1}{R^2} + C_2\frac{1}{R^3}, \quad (9)$$

$$\frac{F_{\text{cyl}}}{A} = \Gamma - \frac{2\kappa c_0}{R} + \frac{\kappa}{2R^2} + D_1\frac{1}{R^3}, \quad (10)$$

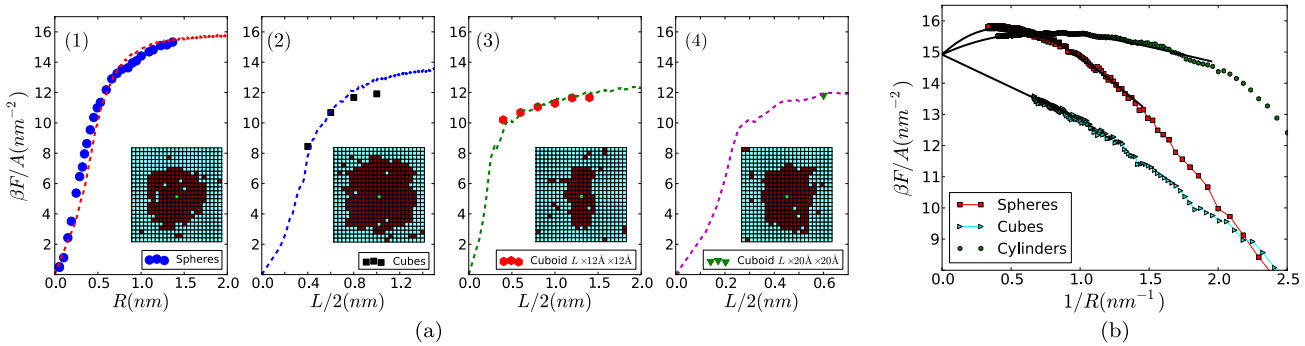

FIG. 2 (color online). (a) Estimates of solvation free energies per unit area of ideal hydrophobic spheres, cubes, and cuboids of various sizes obtained from both the coarse-grained lattice model (lines), Eq. (6), and atomistic simulations of SPC/E [22] water (points). Inset: cross sections of snapshots of lattice gas simulations using Eq. (6). The slowly varying density field n_i is predominantly zero in regions occupied by the solute when the volume of the solute v is large. (b) Fits (solid lines) of Eq. (9) and Eq. (10) to estimates of solvation free energies per unit area of ideal hydrophobic spheres and cylinders from the coarse-grained lattice model. These fits are used to extract the macroscopic interfacial properties, κ, c_0, and δ (see text for description). Γ is estimated by extrapolating estimates of F/A for cubes from the lattice model to $\lim L \to \infty$.

for spherical and cylindrical shapes, respectively. (C_1, C_2, and D_1 are constants determining still more subtle material properties that are not discussed here.) Simultaneously fitting theoretical results for spherical and cylindrical solutes to the form of Eqs. (9) and (10) [see Fig. 2(b)] yields $\kappa = -3.54T$ and $c_0 = 0.29\ \mathrm{nm}^{-1}$ and, therefore, $\delta = 2\kappa c_0/\Gamma = -0.14$ nm. These values are consistent with previous estimates from molecular simulation [34], demonstrating unprecedented success in bridging the length scales associated with hydrophobic effects—from the microscopic linear response of Pratt-Chandler theory to the mesoscopic interfacial deformations described by capillary wave theory and Helfrich-like models [2,16,34].

The ability of such a coarse-grained theory to capture the precise shape dependence of interfacial thermodynamics is striking, given the minimal molecular detail Eq. (6) adds to the generic lattice gas. The lattice model, by itself, cannot in fact produce interfaces with nonzero spontaneous curvature c_0, a consequence of symmetry between liquid and vapor phases in this crude description [35]. Accurately predicted nonzero values of c_0 and δ therefore emerge entirely from the coupling of Gaussian density fluctuations at small scales to the generic interfacial roughness of an Ising model. These mechanical details of the air-water interface, which might appear to reflect geometric intricacies of hydrogen bonding, are thus encoded in the simplest measure of microscopic structure in the bulk liquid, its pair correlation function $g(r)$.

We gratefully acknowledge extremely useful discussions with John D. Weeks, Gerhard Hummer, David Chandler, and David Limmer. This project was supported by the U.S. Department of Energy, Office of Basic Energy Sciences, through the Chemical Sciences Division (CSD) of the Lawrence Berkeley National Laboratory (LBNL), under Contract DE-AC02-05CH11231.

[1] K. R. Mecke and S. Dietrich, Phys. Rev. E **59**, 6766 (1999).
[2] J. D. Weeks, J. Chem. Phys. **67**, 3106 (1977).
[3] D. Chandler, Phys. Rev. E **48**, 2898 (1993).
[4] G. Hummer, S. Garde, A. E. Garcia, A. Pohorille, and L. R. Pratt, Proc. Natl. Acad. Sci. U.S.A. **93**, 8951 (1996).
[5] P. Setny, R. Baron, P. Michael Kekenes-Huskey, J. A. McCammon, and J. Dzubiella, Proc. Natl. Acad. Sci. U.S.A. **110**, 1197 (2013).
[6] M. Cavallaro, L. Botto, E. P. Lewandowski, M. Wang, and K. J. Stebe, Proc. Natl. Acad. Sci. U.S.A. **108**, 20923 (2011).
[7] S. Vaikuntanathan, R. Shaffer, and P. L. Geissler, Faraday Discuss. Chem. Soc. **160**, 63 (2013).
[8] D. E. Otten, P. R. Shaffer, P. L. Geissler, and R. J. Saykally, Proc. Natl. Acad. Sci. U.S.A. **109**, 701 (2012).
[9] Y. Levin, A. P. dos Santos, and A. Diehl, Phys. Rev. Lett. **103**, 257802 (2009).
[10] K. Lum, D. Chandler, and J. D. Weeks, J. Phys. Chem. B **103**, 4570 (1999).
[11] P. R. ten Wolde, S. X. Sun, and D. Chandler, Phys. Rev. E **65**, 011201 (2001).
[12] P. Varilly, A. J. Patel, and D. Chandler, J. Chem. Phys. **134**, 074109 (2011).
[13] P. R. ten Wolde and D. Chandler, Proc. Natl. Acad. Sci. U.S.A. **99**, 6539 (2002).
[14] A. P. Willard and D. Chandler, J. Phys. Chem. B **112**, 6187 (2008).
[15] A. P. Willard and D. Chandler, Faraday Discuss. Chem. Soc. **141**, 209 (2009).
[16] A. J. Patel, P. Varilly, S. N. Jamadagni, H. Acharya, S. Garde, and D. Chandler, Proc. Natl. Acad. Sci. U.S.A. **108**, 17678 (2011).
[17] See Supplemental Material at http://link.aps.org/supplemental/10.1103/PhysRevLett.112.020603 for details of the calculation.
[18] J. Weeks, G. Gilmer, and H. Leamy, Phys. Rev. Lett. **31**, 549 (1973).
[19] S. T. Chui and J. D. Weeks, Phys. Rev. Lett. **40**, 733 (1978).
[20] M. Kardar, *Statistical Physics of Fields* (Cambridge University Press, Cambridge, England, 2007).
[21] S. Vaikuntanathan and P. L. Geissler (unpublished).
[22] H. J. C. Berendsen, J. R. Grigera, and T. P. Straatsma, J. Phys. Chem. **91**, 6269 (1987).
[23] J. J. S. Rowlinson and B. Widom, *Molecular Theory of Capillarity* (Courier Dover, Minola, NY, 2002).
[24] H. N. V. Temperley, Math. Proc. Cambridge Philos. Soc. **48**, 683 (1952).
[25] S. T. Chui and J. D. Weeks, Phys. Rev. B **23**, 2438 (1981).
[26] M. Fisher, J. Stat. Phys. **34**, 667 (1984).
[27] D. Nelson, T. Piran, and S. Weinberg, *Statistical Mechanics of Membranes and Surfaces*, Jerusalem Winter School for Theoretical Physics (World Scientific, Singapore, 2004).
[28] D. G. A. L. Aarts, M. Schmidt, and H. N. W. Lekkerkerker, Science **304**, 847 (2004).
[29] J. Mittal and G. Hummer, Proc. Natl. Acad. Sci. U.S.A. **105**, 20130 (2008).
[30] K. K. Mon, S. Wansleben, D. P. Landau, and K. Binder, Phys. Rev. B **39**, 7089 (1989).
[31] M. Hasenbusch and K. Pinn, Physica (Amsterdam) **192A**, 342 (1993).
[32] M. Schrader, P. Virnau, D. Winter, T. Zykova-Timan, and K. Binder, Eur. Phys. J. Spec. Top. **177**, 103 (2009).
[33] D. M. Huang, P. L. Geissler, and D. Chandler, J. Phys. Chem. B **105**, 6704 (2001).
[34] F. Sedlmeier and R. R. Netz, J. Chem. Phys. **137**, 135102 (2012).
[35] M. P. A. Fisher and M. Wortis, Phys. Rev. B **29**, 6252 (1984).